Journal of Pain Research

Dovepress
open access to scientific and medical research

Open Access Full Text Article

ORIGINAL RESEARCH

Neuropathic Pain Creates Systemic Ultrastructural Changes in the Nervous System Corrected by Electroacupuncture but Not by Pregabalin

Lei Gao[1,2,*]
Jian-Feng Zhang[3,*]
John P Williams[4]
Yi-Ning Yan[1]
Xi-Lai Xiao[1]
Wan-Rui Shi[5]
Xiao-Yan Qian[1]
Jian-Xiong An[1–3,6]

[1]Department of Anesthesiology, Pain and Sleep Medicine, Aviation General Hospital of China Medical University and Beijing Institute of Translational Medicine, Chinese Academy of Sciences, Beijing, People's Republic of China; [2]School of Anesthesiology, Weifang Medical University, Weifang, Shangdong, People's Republic of China; [3]Savaid Medical School, University of Chinese Academy of Sciences, Beijing, People's Republic of China; [4]Department of Anesthesiology, University of Pittsburgh School of Medicine, Pittsburgh, PA, USA; [5]Department of Anesthesiology, Peking University Third Hospital, Beijing, People's Republic of China; [6]School of Medical Science & Engineering, Beijing Advanced Innovation Center for Biomedical Engineering, Beihang University, Beijing, People's Republic of China

*These authors contributed equally to this work

Correspondence: Jian-Xiong An
Department of Anesthesiology, Pain and Sleep Medicine, Aviation General Hospital of China Medical University, Beiyuan Road 3#, Beijing, 100012, People's Republic of China
Tel +86 13801281750
Fax +86 59520233
Email anjianxiong@yeah.net

Purpose: It is unclear whether neuropathological structural changes in the peripheral nervous system and central nervous system can occur in the spared nerve injury model. In this study, we investigated the pathological changes in the nervous system in a model of neuropathic pain as well as the effects of electroacupuncture (EA) and pregabalin (PGB) administration as regards pain relief and tissue repair.

Patients and Methods: Forty adult male SD rats were equally and randomly divided into 4 groups: spared nerve injury group (SNI, n = 10), SNI with electroacupuncture group (EA, n = 10), SNI with pregabalin group (PGB, n =10) and sham-operated group (Sham, n=10). EA and PGB were given from postoperative day (POD) 14 to 36. EA (2 Hz and 100 Hz alternating frequencies, intensities ranging from 1–1.5–2 mA) was applied to the left "zusanli" (ST36) and "Yanglingquan" (GB34) acupoints for 30 minutes. The mechanical withdrawal thresholds (MWTs) were tested with von Frey filaments. Moreover, the organizational and structural alterations of the bilateral prefrontal cortex, hippocampus, sciatic nerves and the thoracic, lumbar spinal cords and dorsal root ganglions (DRGs) were examined via light and electron microscopy.

Results: MWTs of left hind paw demonstrated a remarkable decrease in the SNI model ($P < 0.05$). In the SNI model, ultrastructural changes including demyelination and damaged neurons were observed at all levels of the peripheral nervous system (PNS) and central nervous system (CNS). In addition, EA improved MWTs and restored the normal structure of neurons. However, the effect was not found in the PGB treatment group.

Conclusion: Chronic pain can induce extensive damage to the central and peripheral nervous systems. Meanwhile, EA and PGB can both alleviate chronic pain syndromes in rats, but EA also restores the normal cellular structures, while PGB is associated with no improvement.

Keywords: neuropathic pain, structural changes, electroacupuncture, pregabalin

Introduction

Neuropathic pain (NP) is a particularly intractable and persistent type of chronic pain that arises as a direct consequence of a pathological insult to the somatosensory system.[1] The pain is characterized by shooting or burning quality, hyperalgesia, allodynia, numbness, and can occur spontaneously.[2] The prevalence of NP is 9.8% in the general population, and is an important public health issue.[3] Moreover, if this is not treated relatively quickly, it can easily contribute to both depressive and anxiety-like complications as well as chronic cognitive changes. It also poses an incredible burden on not only individuals but also the health care system.[4]

Received: 9 June 2021
Accepted: 28 August 2021
Published: 14 September 2021

Unfortunately, management of NP remains a major clinical challenge, given that the pathogenesis of NP is not yet completely elucidated.[5] Moreover, regardless of the inciting cause of NP it always shares the clinical characteristics previously described.[6] We speculated that a central nervous system (CNS) injury may be associated with these characteristics in patients with NP. It is therefore crucial to the further understanding of the pathophysiology of NP to investigate possible mechanisms and patterns of injury and their treatment.

Available clinical neuroimaging evidence indicates that chronic pain is considered a CNS disorder.[7] Several brain regions are activated in response to nociceptive stimulation, such as the raphe and the periaqueductal gray, the primary and secondary somatosensory cortices, thalamus, insula, and the mid-cingulate cortex (MCC).[8,9] Wang et al have observed reductions in the gray matter volume of many cortical and subcortical cerebral areas in trigeminal neuralgia (TN) patients.[10] Previous basic research from our team has confirmed that rats with an experimental TN lesion exhibit systemic ultrastructural changes in the prefrontal cortex (PFC), hippocampus and medulla oblongata.[11–13] Electro-acupuncture (EA) can restore many if not most of these ultrastructural changes, while pregabalin (PGB) does not show equivalent improvement.[11] Despite significant research efforts, detailed knowledge about the pathophysiology involved and the structural and functional changes of the CNS induced by NP is still limited.

In the present study, we aimed to demonstrate the pathophysiology underlying the systemic ultrastructural changes of the nervous systems induced by neuropathic pain. In addition, the effects of EA intervention and PGB administration in pain relief and tissue repair were also assessed.

Materials and Methods

Ethical Statement

All animal experimental procedures were approved by the Animal Research Ethics Committee of Aviation General Hospital of Medical University and were performed in accordance with the ethical guidelines for the Care and Use of the International Association for the Study of Pain.[14]

Animals

Forty adult male Sprague-Dawley rats, weighing 250–300g, were purchased from Beijing Vital River Laboratory Animal Technology (Beijing, People's Republic of China). Rats were housed in groups of four in plastic cages under standard laboratory conditions (22 ± 2°C, 12 h light/dark cycles and 50–70% relative humidity). Food and water were available ad libitum. Rats were divided into four groups randomly: spared nerve injury group (SNI, n=10), electro-acupuncture group (EA, n = 10), pregabalin group (PGB, n =10) and sham-operated group (Sham, n=10).

Spared Nerve Injury (SNI) Sciatic Neuralgia Rat Model Establishment

The SNI model was established as previously described.[15] The rats were anesthetized using 1% Pelltobarbitalum Natricum (40 mg/kg body weight intraperitoneally, AMRESCO, USA). Then, blunt dissection was performed to expose the three peripheral nerve branches of the left sciatic nerve. The common peroneal and tibial nerves were tightly ligated by 5.0 silk and 2–4 mm portion of the nerves was removed. The sural nerve remained intact and great care was taken to avoid any contact with or stretching of this nerve. In the sham operation, the animals received the same procedure but without any lesion to the sciatic nerve.

Behavioral Assessments

Animals were tested 3 days before the surgery and on 3, 6, 9, 12, 15, 20, 25, 30, and 40 days after the surgery. Testing was performed from 7 am to 7 pm. Rats were placed in transparent plastic boxes (20×20×20 cm) on an elevated metal mesh floor. A habituation of 15–30 min was allowed before the test. Then, the threshold for paw withdrawal (both ipsilateral and contralateral sides) was stimulated with calibrated von Frey monofilaments (Stoelting, Chicago, IL).[16] Monofilaments were perpendicularly applied to the glabrous area of limbs with adequate force to cause filament bending. A sharp withdrawal of the paw was considered as a positive response. Behavioral testing was also done at the same time each day.

PGB Administration

PGB (75 mg, Pfizer, New York, NY) was dissolved in 7.5mL 0.9% saline and administered by oral gavage using an intragastric instrument. Previously, it was shown that PGB reduced the nociceptive response after chronic contractile injury (CCI) of the sciatic nerve in a dose-dependent manner (3–30 mg/kg). Therefore, PGB treatment (30mg/kg) started from the 14th day following

surgery and continued for 23 days, from postoperative day 14 to 36.[17] PGB administration occurred at the same time each day to avoid possible circadian effects.

EA Intervention

According to the procedure described by Tao et al,[18] the rats were treated with EA starting on the 14th day after surgery. During the treatment, disposable intradermal acupuncture needles (gauge #32, 0.5 in length) were inserted into the left hind paw "Zusanli" (ST36) and "Yanglingquan" (GB34).[19] " Yanglingquan" (GB34) is anatomically located along the outer side of the lower leg, in the depression anterior and inferior to the fibular head.[20] "Zusanli" (ST36) is located 5 mm below the capitulum fibulae, laterally and posterior to the knee joint.[21] The needle was fixed with adhesive tape and the animal transferred to a transparent plastic cage. EA stimulation was subsequently performed using a Han's Acupoint Nerve Stimulator (HANS, LH series, Peking University). The frequency of EA stimulation remained 2/100 Hz variable, and the current intensity remained at 1 mA for 10 minutes, then increased to 1.5 mA for 10 minutes, and finally increased to 2 mA for 10 minutes. EA treatment was performed once every 3 days for 30 minutes, from 14 to 36 days after surgery and conducted at the same time each day.

Morphology Studies

On day 40 after surgery, the experimental animals in the four groups (Sham, SNI, EA, and PGB group) were sacrificed and tissue samples were prepared. In brief, tissue samples of the spinal cord (T_7 and L_4 level) and brain were removed and fixed in 10% neutral formalin fixative for 48 h. Then, these tissue samples were embedded in paraffin wax. Paraffin-embedded tissue was cut into 5 micron thick sections and histologically examined using H&E staining and Nissl staining for general assessment of histopathological changes.[22]

Transmission Electron Microscopy (TEM)

The preparation of samples was described previously.[11] Under deep anesthesia, animals were perfused with warm saline, solution of 4% paraformaldehyde and 2% glutaraldehyde (Sigma, St. Louis, Missouri, USA). The bilateral prefrontal cortex, hippocampus, bilateral sciatic nerves, the spinal cord and dorsal root ganglions (DRGs) at the thoracic (T7), and lumbar (L4) levels were immersed in 3% glutaraldehyde for 24 hours, and then washed 3 times with 0.1M phosphate buffer. The tissues were fixed with 1% osmium tetroxide (Sigma, St. Louis, MO, USA) for 2 hours, dehydrated, embedded in araldite, cut into 1 μm plastic sections and stained with uranyl acetate and then observed under a Hitachi H-7700 transmission electron microscope (Hitachi Ltd., Tokyo, Japan).

Statistical Analysis

All statistical analyses were performed using SPSS Version 24.0 (IBM Corporation, NY, United States). All data are presented as the mean ± standard deviation (SD). Comparisons between groups were performed using one-way analysis of variance (ANOVA). Comparisons of intra-group differences across time were assessed with repeated measures analysis and $p < 0.05$ was considered as statistically significant.

Results

SNI Induced Behavioral Signs of Nociception in the Hind Paw

As shown in Figure 1, there were no significant differences in mechanical withdrawal thresholds (MWTs) between the 4 groups prior to surgery. However, the MWT of the SNI group showed a significant decrease after operation in comparison to the sham group. Compared with the SNI group, there were no significant differences in MWT of the non-operative hind paw between the EA and PGB groups. The MWTs on the operative hind paw of the SNI model group showed significant decreases after operation in comparison to the sham group ($^{*}p < 0.05$). We observed that EA treatment starting 14 days after surgery increased the MWTs of the operative hind paw to von Frey stimulation. Significant recovery was first observed after 7 days of treatment with EA ($^{-}p = 0.015$). The recovery effect continued until the end of the experimental period. Similar effects were observed in the PGB treatment group ($^{\#}p = 0.021$). Therefore, both EA and PGB treatment reduced the behavioral effects associated with sciatic nerve injury.

Neuropathological Changes of Nervous Systems in Rat with SNI

H&E and Nissl staining demonstrated no obvious pathological change in the sham group in bilateral prefrontal cortex and hippocampus. The cell boundaries were clear and closely arranged with clear nuclei in bilateral prefrontal cortex (Figure 2A, C, a and c) and hippocampus (Figure 2E, G, e and g). In comparison, the bilateral

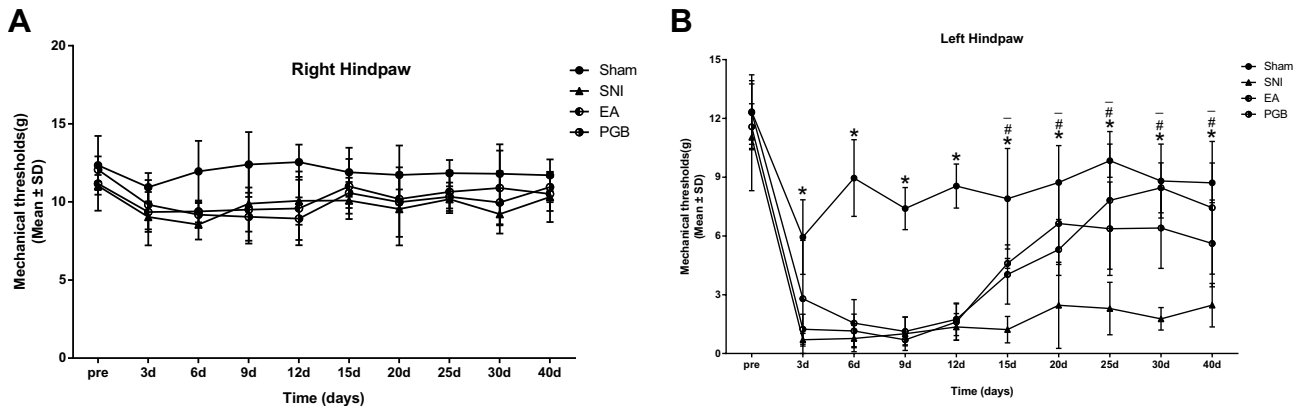

Figure 1 MWTs between four groups for hind paw at different time intervals.
Notes: The changes of MWTs between right hind paw (**A**) and left hind paw (**B**) were compared. There were no significant differences in the MWTs prior to treatments ($P = 0.095$). Compared with the sham operation group, there was no significant difference in MWT of the right rear claw among the three groups (SNI group, EA group and PGB group). The MWTs of the SNI model group for left hind paw had a remarkable decrease after operation in comparison to the sham-operated group (*compared between SNI group and the sham-operation group, $*P < 0.05$). For the EA and PGB groups, the MWTs of left hind paw had obvious increase after EA and PGB intervention ($^{\#}$, ¯compared between PGB and EA with SNI, $^{\#}P < 0.05$, ¯$P < 0.05$,). Error bars indicate the standard deviation. Data are presented as mean ± SD, $^{\#}$, ¯$P < 0.05$.
Abbreviations: MWTs, mechanical withdrawal thresholds; SNI, spared nerve injury; EA, electroacupuncture; PGB, pregabalin.

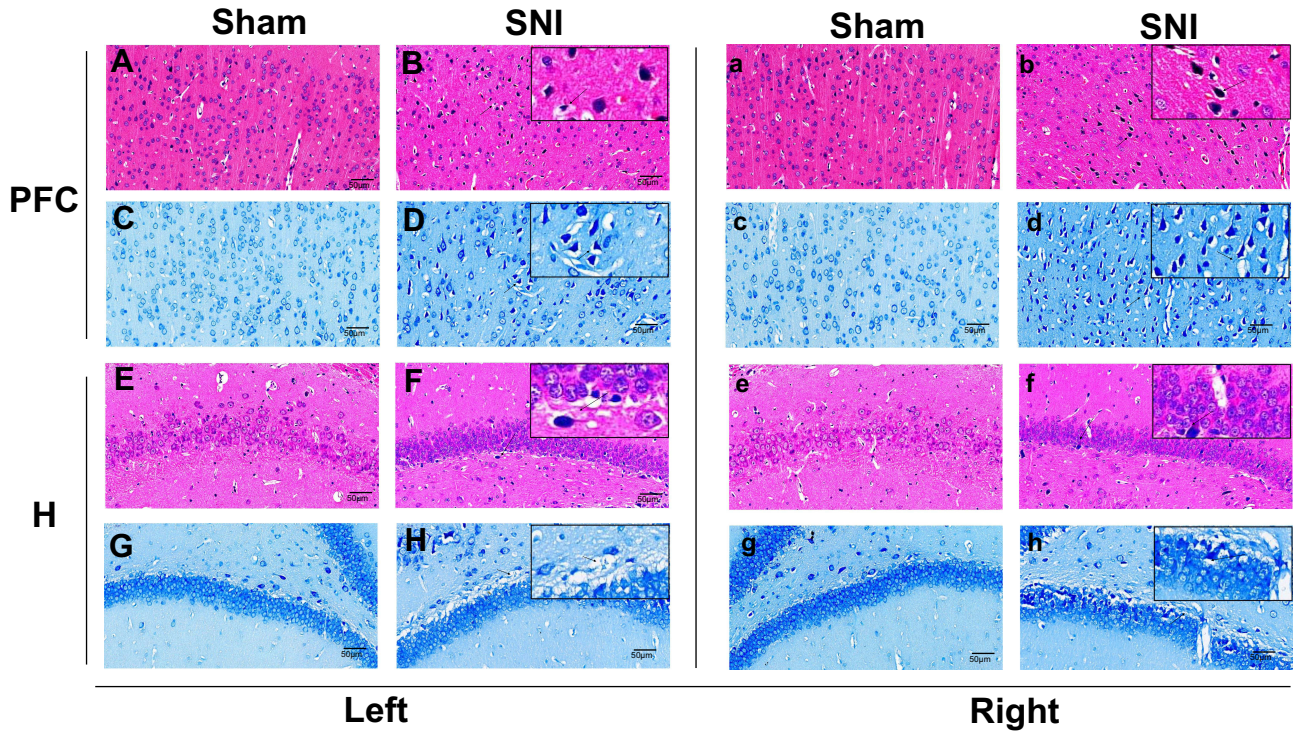

Figure 2 Hematoxylin and eosin (H&E) stained and Nissl-stained sections from bilateral prefrontal cortex and hippocampus in sham-operated and SNI group.
Notes: The cell boundaries of bilateral prefrontal cortex (**A, a, C, c**) and hippocampus (**E, e, G, g**) were clear and closely arranged with clear nuclei in sham-operated group. The prefrontal cortex (**B, b, D, d**) and hippocampus (**F, f, H, h**) of the SNI group revealed disorderly arrangement of neurons, irregularly shaped neurons with shrunken cell bodies, ruptured nuclear membranes and vanishing nucleolus. The arrows show irregularly shaped neurons with shrunken cell body, ruptured nuclear membranes and disappeared nucleolus. (**A, a, C, c**) Morphological alterations of the prefrontal cortex in sham-operated group. (**A** and **C**) H&E and Nissl staining of ipsilateral (left side) prefrontal cortex respectively. And (**a** and **c**) represent the H&E and Nissl staining of contralateral (right side) prefrontal cortex respectively. (**B, b, D, d**) Structural changes of the prefrontal cortex in SNI group. (**B** and **D**) H&E and Nissl staining of ipsilateral (left side) prefrontal cortex respectively. (**b** and **d**) H&E and Nissl staining of contralateral (right side) prefrontal cortex respectively. Similarly, (**E, e, G, g**) show the H&E and Nissl staining of bilateral hippocampus in sham-operated group. (**F, f, H, h**) H&E and Nissl staining of bilateral hippocampus in SNI group.
Abbreviations: SNI, spared nerve injury; EA, electroacupuncture; PGB, pregabalin; PFC, prefrontal cortex; H, hippocampus.

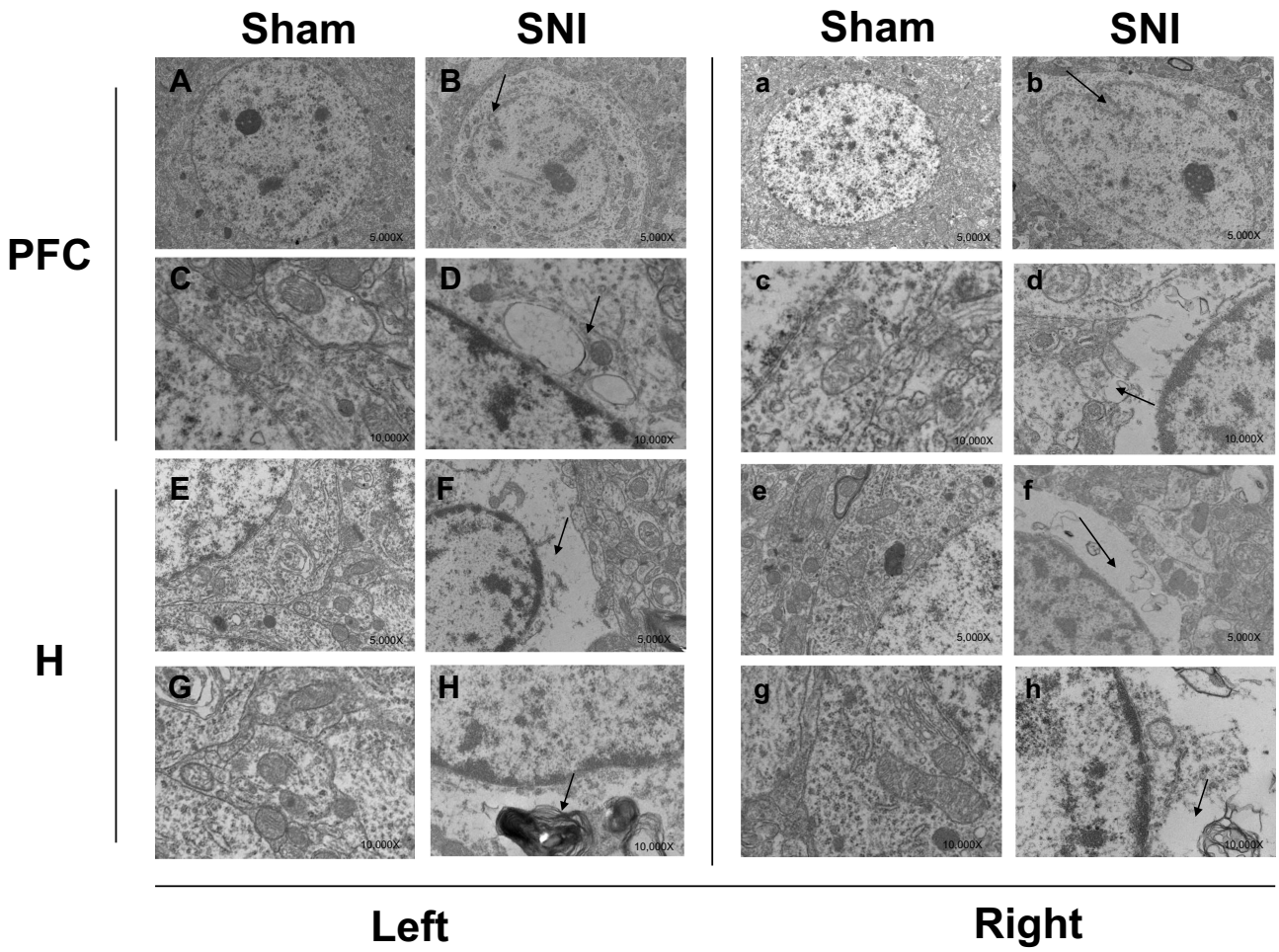

Figure 3 Ultrastructural changes of bilateral prefrontal cortex and hippocampus in sham-operated and SNI group.
Notes: Normal appearing endoplasmic reticulum, Golgi body, intact outer nuclear membranes and mitochondria are observed in bilateral prefrontal cortex (**A, a, C, c**) and hippocampus (**E, e, G, g**) in sham-operated group. Meanwhile, the prefrontal cortex (**B, b, D, d**) and hippocampus (**F, f, H, h**) of the SNI group revealed abnormal indentation of neurons, damaged mitochondria and Golgi apparatus, and dissolving surrounding tissues. (**A, a, C, c**), demonstrate the ultrastructural alterations of the prefrontal cortex in sham-operated group. (**A** and **C**) represent the ipsilateral (left side) prefrontal cortex respectively. While (**a** and **c**) represent contralateral (right side) prefrontal cortex respectively. (**B, b, D, d**) show the ultrastructure changes of the prefrontal cortex in SNI group. (**B** and **D**) represent ipsilateral (left side) prefrontal cortex respectively. And (**b** and **d**) represent the H&E and Nissl staining of contralateral (right side) prefrontal cortex respectively. Similarly, (**E, e, G, g**) show the bilateral hippocampus in sham-operated group. (**F, f, H, h**) represent the bilateral hippocampus in SNI group.
Abbreviations: SNI, spared nerve injury; EA, electroacupuncture; PGB, pregabalin; PFC, prefrontal cortex; H, hippocampus.

prefrontal cortex and hippocampus of the SNI group revealed disorderly arrangement of neurons, irregularly shaped neurons with shrunken cell bodies, ruptured nuclear membranes and vanishing nucleolus (prefrontal cortex: Figure 2B, D, b and d; hippocampus: Figure 2F, H, f and h). Similarly, TEM in the sham group showed normal neurons in the bilateral prefrontal cortex (Figure 3A, C, a and c) and hippocampus (Figure 3E, G, e and g) with normal appearing endoplasmic reticulum, Golgi body, intact outer nuclear membranes and mitochondria. Compared with the sham group, the SNI group showed abnormal indentation of neurons, damaged mitochondria and Golgi apparatus, and dissolving surrounding tissues in the bilateral prefrontal cortex (Figure 3B, D, b and d) and hippocampus (Figure 3F, H, f and h).

As for the pathological changes of different levels of the spinal cord, the rats in the SNI model group showed cell nuclei contraction in the bilateral thoracic spine (Figure 4B, D, b and d) and lumbar spinal cord (Figure 4F, H, f and h), neurons disappeared into vacuoles, and Nissl bodies were deeply stained and partially lost compared with the sham operation group (thoracic spine: Figure 4A, C, a and c; lumbar spinal cord: Figure 4E, G, e and g). TEM observations demonstrated a light demyelination in both the operative (thoracic spinal cord: Figure 5D; thoracic DRG: 5B; lumbar spinal cord:

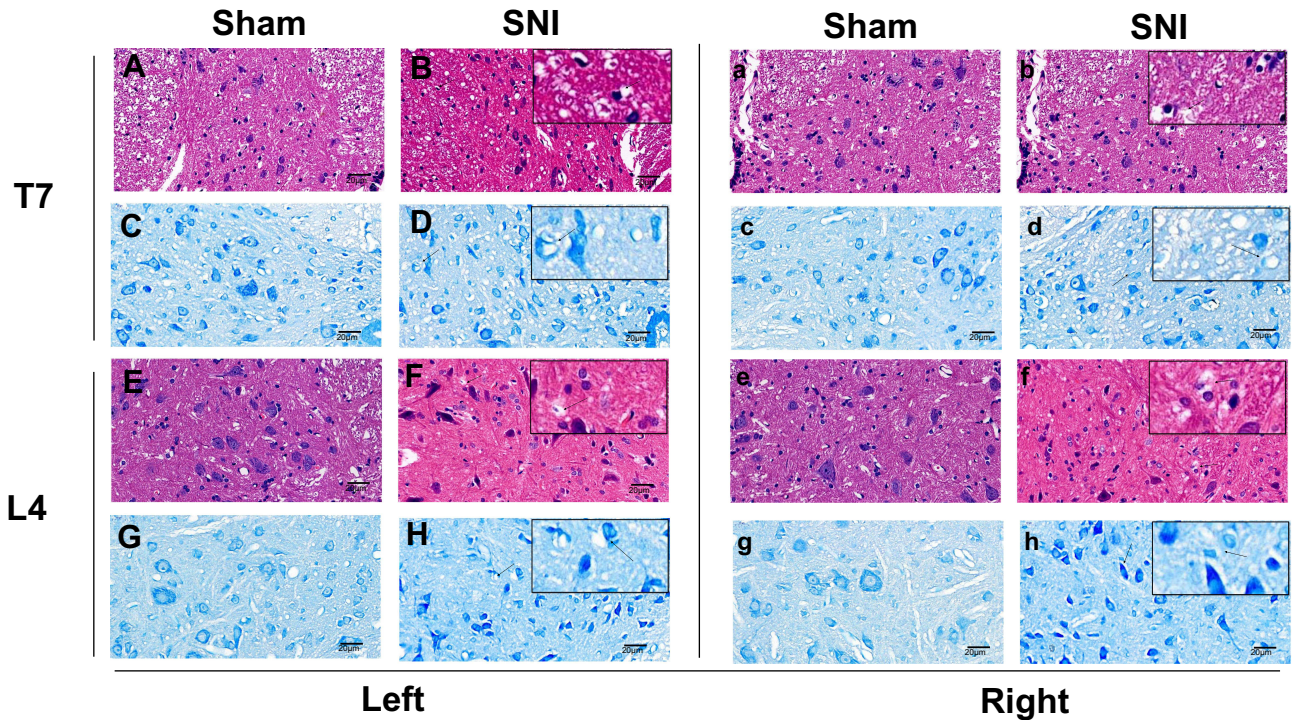

Figure 4 H&E and Nissl-stained sections from thoracic and lumbar spinal cords.
Notes: In sham-operated group, normal cell structures are observed in thoracic spine (**A, a, C, c**) and lumbar spinal cord (**E, e, G, g**). Cell nuclei contraction and neurons disappeared into vacuoles are observed in thoracic spine (**B, b, D, d**) and lumbar spinal cord (**F, f, H, h**) in SNI group. (**A, a, C, c**), demonstrate the neuropathological alterations of the thoracic spine in sham-operated group. (**A** and **C**) represent the H&E and Nissl staining of ipsilateral (left side) thoracic spine respectively. And (**a** and **c**) represent the H&E and Nissl staining of contralateral (right side) thoracic spine respectively. (**B, b, D, d**) show the structural changes of the thoracic spine in SNI group. (**B** and **D**) represent the H&E and Nissl staining of ipsilateral (left side) thoracic spine respectively. (**b** and **d**) represent the H&E and Nissl staining of contralateral (right side) thoracic spine respectively. Similarly, (**E, e, G, g**) show the H&E and Nissl staining of bilateral lumbar spinal cord in sham-operated group. (**F, f, H, h**) represent the H&E and Nissl staining of bilateral lumbar spinal cord in SNI group.
Abbreviations: SNI, spared nerve injury; EA, electroacupuncture; PGB, pregabalin; T7, the 7th thoracic spine; L4, the 4th lumbar spinal cords.

Figure 5H; lumbar DRG: 5F) and non-operative spinal cords and DRGs (thoracic spinal cord: Figure 5d; thoracic DRG: 5b; lumbar spinal cord: Figure 5h; lumbar DRG: 5f) at thoracic, and lumbar levels in SNI group rats compared with sham operation group (thoracic spinal cord: Figure 5C and c; thoracic DRGs: 5A and a; lumbar spinal cord: Figure 5G and g; lumbar DRGs: 5E and e) on POD 40. As expected, the spared nerve injury caused damage to the spinal cord DRGs at all levels examined. The myelin sheaths were swollen, twisted and showed demyelination on both the operative and non-operative sides.

Similar phenomenon has been observed in sciatic nerve. On postoperative day 40, complete and clearly visible myelin sheaths were observed on the operative (Figure 5I) and non-operative (Figure 5i) sciatic nerve in the sham group. In the SNI group, demyelination and Schwann cell degeneration were noted in the operative sciatic nerve (Figure 5J). Similarly, damage was observed in the contralateral sciatic nerve (Figure 5j).

EA but Not PGB Treatment Restored Normal Structures of the Nervous Systems

After EA treatment, cell atrophy and nucleolar loss were reduced in the bilateral prefrontal cortex (Figure 6A, a, C and c) and hippocampus (Figure 6E, e, G and g). However, in PGB group, many cytoplasmic inclusions and nuclear shrinkage appeared in the bilateral hippocampus (Figure 6F, f, H and h) and prefrontal cortex (Figure 6B, b, D and d). Cells exhibited a disorderly arrangement, and neuronal eosinophilia was present. TEM observation showed intact and normal neuronal cells in the bilateral prefrontal cortex (Figure 7A, a, C and c) and hippocampus (Figure 7E, e, G and g), as well as intact endoplasmic reticulum and mitochondrial membranes in EA group. However, in the PGB treatment group, damage in the bilateral hippocampal (Figure 7F, f, H and h) and prefrontal cortex (Figure 7B, b, D and d) did not show similar improvement. Partial cytoplasmic lysis and changes in neuronal cell bodies and mitochondria were still present.

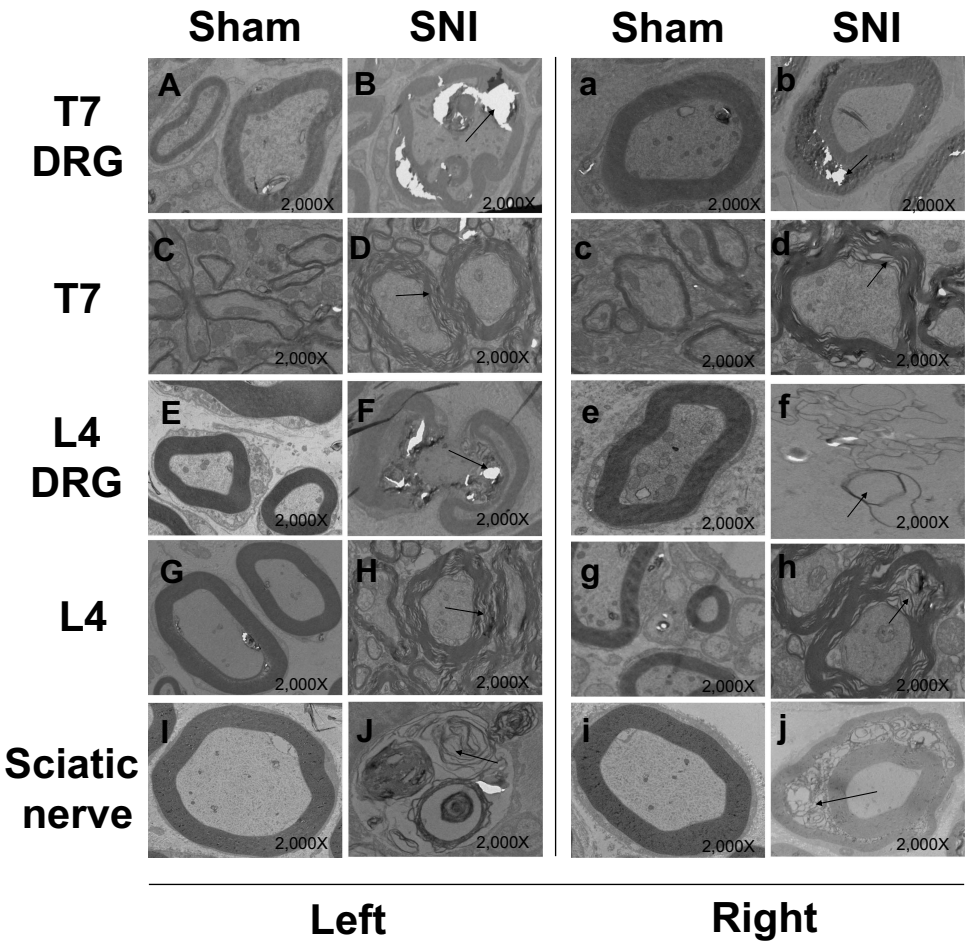

Figure 5 Ultrastructural changes of thoracic and lumbar spine, DRGs and sciatic nerves in SNI group compared with sham-operated group.
Notes: Complete and clearly visible myelin sheaths are observed in bilateral thoracic and lumbar spine, DRGs and sciatic nerves in sham-operated group (**A, a, C, c, E, e, G, g, I, i**). While the myelin sheaths were destroyed in SNI group (**B, b, D, d, F, f, H, h, J, j**). (**A, a, C, c, E, e, G, g, I, I**) show the ultrastructural changes of thoracic and lumbar spine, DRGs and sciatic nerves in sham-operated group. (**A, C, E, G, I**) represent the left side (operative side). While **a, c, e, g, I** represent the right side (non-operative side). (**B, b, D, d, F, f, H, h, J, j**) represent the ultrastructural changes of thoracic and lumbar spine, DRGs and sciatic nerves in SNI group. (**B, D, F, H, J**) represent the left side (operative side). While (**b, d, f, h, j**) represent the right side (non-operative side).
Abbreviations: SNI, spared nerve injury; EA, electroacupuncture; PGB, pregabalin; T7, the 7th thoracic spine; L4, the 4th lumbar spinal cords; DRG, dorsal root ganglion.

Similarly, H&E and Nissl staining demonstrated that the spinal cord tissue of the EA group showed no obvious neuronal damage in bilateral thoracic spine (Figure 8A, a, C and c) and bilateral lumbar spinal cord (Figure 8E, e, G and g), while those in the PGB group (thoracic spine: Figure 8B, b, D and d; lumbar spinal cord: 8F, f, H and h) showed no obvious improvement in neuronal damage compared to the rats in the SNI group. In addition, TEM observations also showed that myelin sheaths on the operative (thoracic spinal cord: Figure 9C; thoracic DRG: 9A; lumbar spinal cord: Figure 9G; lumbar DRG: 9E) and non-operative (thoracic spinal cord: Figure 9c; thoracic DRG: 9a; lumbar spinal cord: Figure 9g; lumbar DRG: 9e) thoracic, lumbar spinal cords levels and DRGs were intact and normal in EA treated rats. However, in PGB-treated rats, operative (thoracic spinal cord: Figure 9D; thoracic DRG: 9B; lumbar spinal cord: Figure 9H; lumbar DRG: 9F) and non-operative (thoracic spinal cord: Figure 9d; thoracic DRG: 9b; lumbar spinal cord: Figure 9h; lumbar DRG: 9f) side DRGs showed partial myeloid dissolution and onion-like demyelinating changes. As for bilateral sciatic nerve, slight demyelination was observed in EA group (Figure 9I and i) compared to SNI group. However, severely swollen myelin sheaths were shown in the PGB group (Figure 9J and j).

Discussion

Generally, a better rodent animal model is the premise and foundation for elucidating the mechanism of NP and evaluating potential treatment. The current mainstream models

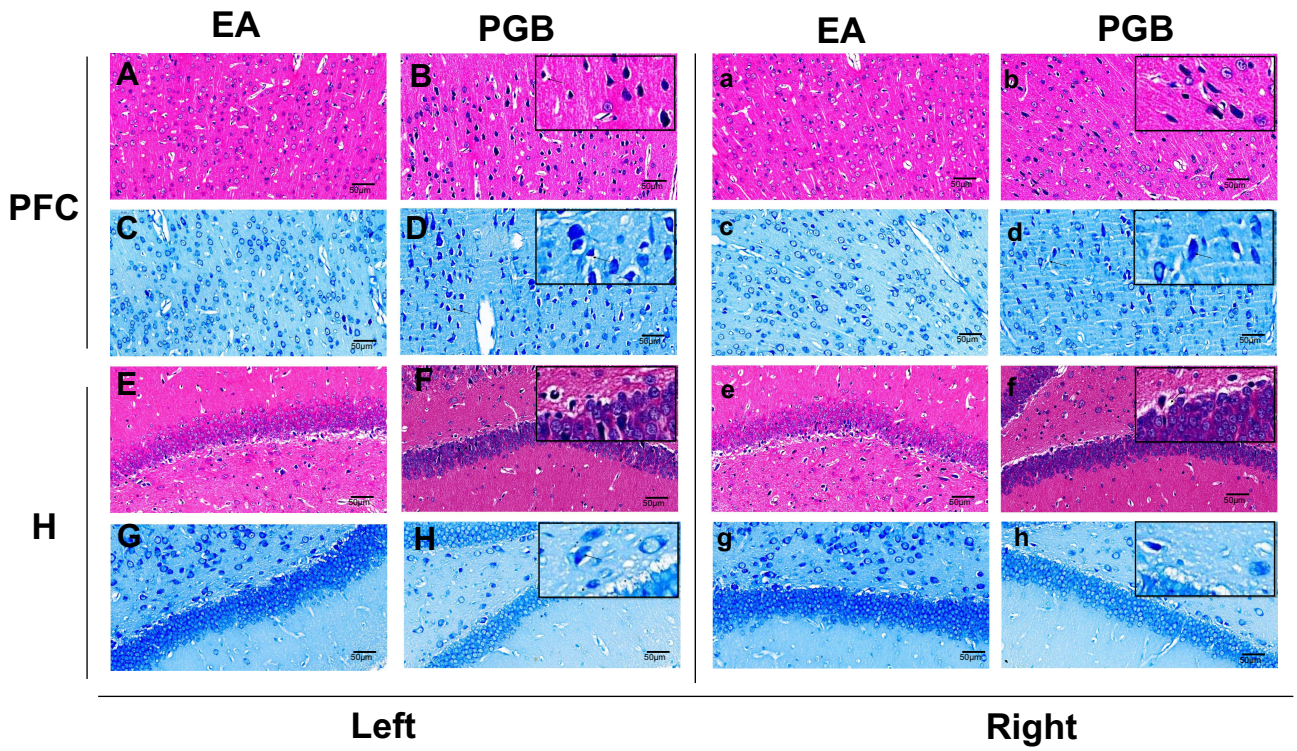

Figure 6 Effects of EA and PGB in neuropathological alterations of bilateral prefrontal cortex and hippocampus.
Notes: Cell atrophy and nucleolar loss were reduced in the bilateral prefrontal cortex (**A, a, C, c**) and hippocampus (**E, e, G, g**) after EA treatment. Many cytoplasmic inclusions and nuclear shrinkage still appeared in the prefrontal cortex (**B, b, D, d**) and hippocampus (**F, f, H, h**) in PGB group. (**A, a, C, c**), demonstrate the morphological alterations of the prefrontal cortex in EA group. (**A** and **C**) represent the H&E and Nissl staining of ipsilateral (left side) prefrontal cortex respectively. And **a** and **c** represent the H&E and Nissl staining of contralateral (right side) prefrontal cortex respectively. (**B, b, D, d**) show the structural changes of the prefrontal cortex in PGB group. (**B** and **D**) represent the H&E and Nissl staining of ipsilateral (left side) prefrontal cortex respectively. (**b** and **d**) represent the H&E and Nissl staining of contralateral (right side) prefrontal cortex respectively. Similarly, (**E, e, G, g**) show the H&E and Nissl staining of bilateral hippocampus in EA group. (**F, f, H, h**) represent the H&E and Nissl staining of bilateral hippocampus in PGB group.
Abbreviations: SNI, spared nerve injury; EA, electroacupuncture; PGB, pregabalin; PFC, prefrontal cortex; H, hippocampus.

for NP include CCI,[23] spinal nerve ligation model (SNL),[24] and SNI.[15] Of which, the SNI rat model is one of the most widely used in the study of NP. In recent years, many studies have used the SNI model to explore the mechanism of NP and innovative therapies.[25–27]

In this study, we found that the systemic ultrastructural alterations were observed at different levels of the nervous system in the SNI rat model. That is, the micro-structure of the bilateral PFC, hippocampus, spinal cord (T_7 and L_4 level), DRGs, and sciatic nerves were damaged in SNI group. Specifically, the shrunken cell bodies, ruptured nuclear membranes and vanishing nucleolus were observed bilaterally in the prefrontal cortex and hippocampus. Meanwhile, the neuropathological changes (mainly demyelination) were also observed at different levels of the spinal cord, bilateral DRGs, and bilateral sciatic nerves. This phenomenon was similar to that seen in our previous studies.[17] We surmise that one of the main causes of this phenomenon is neuroinflammation.

Chronic pain is associated with neuroinflammation.[28] Several lines of evidence suggest that the mechanical allodynia induced by SNI is secondary to a neuroinflammatory response in the CNS, that is characterized by aberrant microglial activation in the spinal cord.[29,30] Gordh et al also reported that patients with severe peripheral neuropathic pain demonstrated upregulation of several chemokines in their cerebrospinal fluid.[31] Neuroinflammation plays an essential role in the generation of central sensitization which is a major contributing factor to the development and maintenance of chronic pain.[32] Neuroinflammation occurred in the peripheral nervous system (PNS) and CNS and was characterized by the infiltration of leukocytes as well as increased production of inflammatory mediators. These inflammatory mediators could lead to demyelination and by neuronal injury by exerting cytotoxic effects on oligodendrocytes and neurons.[33]

Demyelination in nervous systems is a key mechanism in the development of plasticity in neuropathic pain.[34] This

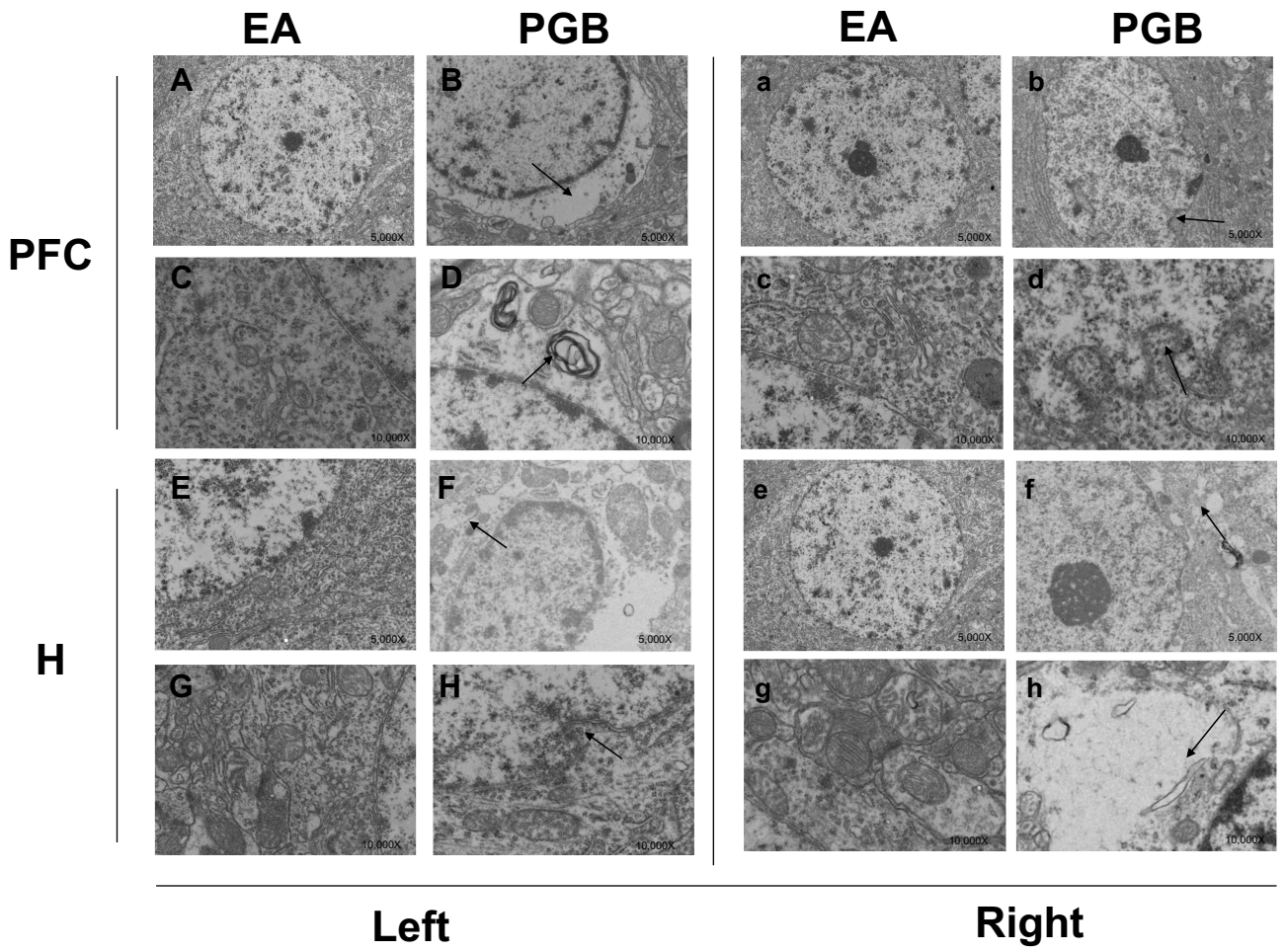

Figure 7 Ultrastructural changes of bilateral prefrontal cortex and hippocampus in EA and PGB group.
Notes: Intact and normal neuronal cells in the bilateral prefrontal cortex (**A, a, C, c**) and hippocampus (**E, e, G, g**), as well as intact endoplasmic reticulum and mitochondrial membranes are observed in EA group. However, damage in the hippocampal (**F, f, H, h**) and prefrontal cortex (**B, b, D, d**) did not show similar improvement. (**A, a, C, c**), demonstrate the ultrastructural alterations of the prefrontal cortex in EA group. (**A** and **C**) represent the ipsilateral (left side) prefrontal cortex respectively. While (**a** and **c**) represent contralateral (right side) prefrontal cortex respectively. (**B, b, D, d**) show the ultrastructural changes of the prefrontal cortex in PGB group. (**B** and **D**) represent ipsilateral (left side) prefrontal cortex respectively. And (**b** and **d**) represent the H&E and Nissl staining of contralateral (right side) prefrontal cortex respectively. Similarly, (**E, e, G, g**) show the bilateral hippocampus in EA group. (**F, f, H, h**) represent the bilateral hippocampus in PGB group.
Abbreviations: SNI, spared nerve injury; EA, electroacupuncture; PGB, pregabalin; PFC, prefrontal cortex; H, hippocampus.

may also explain why ultrastructural alterations were observed bilaterally in tissues in the CNS. As for pathological changes in the PNS, we identified both demyelination and Schwann cell degeneration bilaterally in the sciatic nerve that was not in line with our expectations.

It was easy to understand why the left sciatic nerve (operative side) showed demyelination and Schwann cell degeneration that is expected with the peripheral mechanisms of neuropathic pain.[34] However, a similar damage pattern appeared in the right sciatic nerve (non-operative side). This phenomenon is in line with previous studies[35–38] that suggest a systemic inflammatory response appears to be associated with this phenomenon. Kleinschnitz[35] et al demonstrated interleukin-10 (IL-10), monocyte chemoattractant protein-1 (MCP-1), and IL-1 beta in the contralateral sciatic nerve are significantly increased following unilateral sciatic nerve injury. Another two possible mechanisms have been proposed by Koltzenburg et al.[36] The first is that the contralateral effects are mediated by circulating factors. After unilateral nerve injury, the breakdown products from the denervated tissue and damaged nerve might circulate and induce alterations in the contralateral neuronal populations. The second possibility is that the contralateral effects are mediated by transmedian sprouting. That is, unilateral nerve injury could result in collateral sprouting. Such sprouting could cause the changes in contralateral neurons.

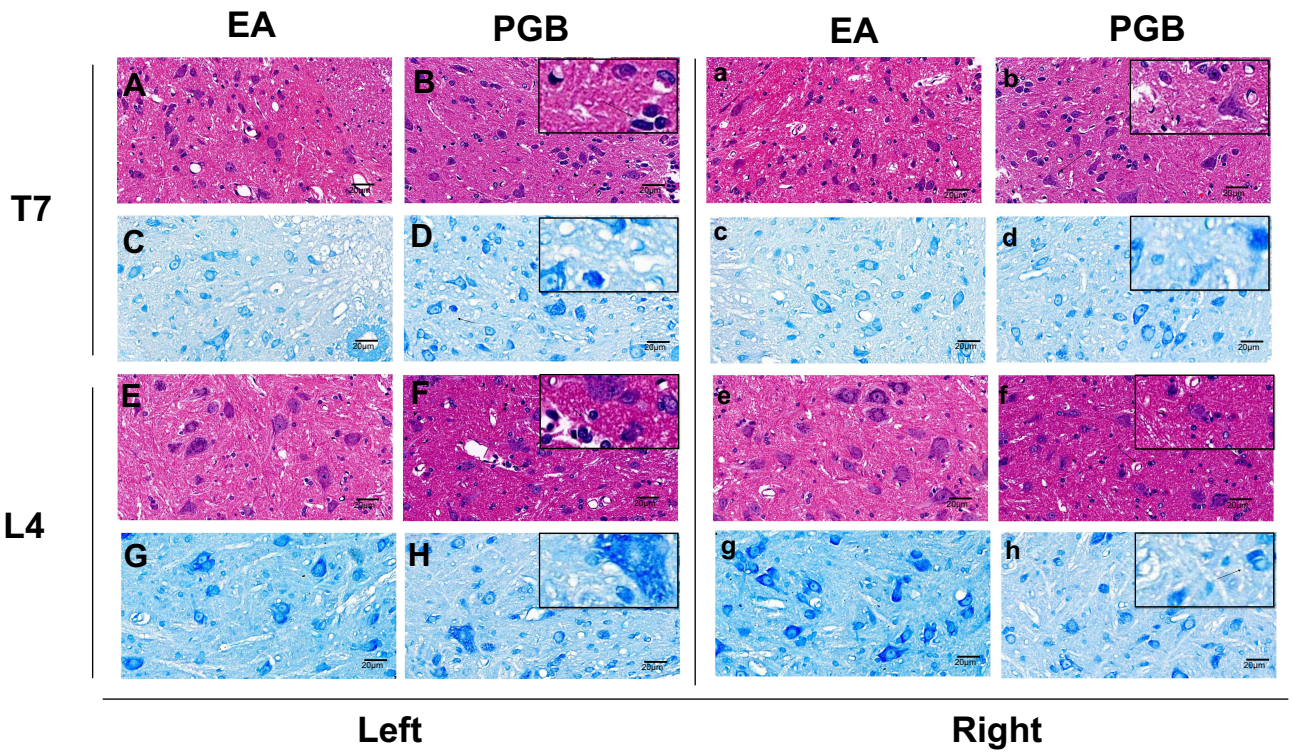

Figure 8 Effects of EA and PGB in neuropathological alterations of bilateral thoracic and lumbar spinal cords.
Notes: Repair of previous damage is evident in EA group (thoracic spine: **A, a, C, c**; lumbar spine: **E, e, G, g**), while PGB is associated with no improvement (thoracic spine: **B, b, D, d**; lumbar spine: **F, f, H, h**). (**A, a, C, c**), demonstrate the neuropathological alterations of the thoracic spine in EA group. (**A** and **C**) represent the H&E and Nissl staining of ipsilateral (left side) thoracic spine respectively. And (**a** and **c**) represent the H&E and Nissl staining of contralateral (right side) thoracic spine respectively. (**B, b, D, d**) show the structural changes of the thoracic spine in PGB group. (**B** and **D**) represent the H&E and Nissl staining of ipsilateral (left side) thoracic spine respectively. (**b** and **d**) represent the H&E and Nissl staining of contralateral (right side) thoracic spine respectively. Similarly, (**E, e, G, g**) show the H&E and Nissl staining of bilateral lumbar spinal cord in EA group. (**F, f, H, h**) represent the H&E and Nissl staining of bilateral lumbar spinal cord in PGB group.
Abbreviations: SNI, spared nerve injury; EA, electroacupuncture; PGB, pregabalin; T7, the 7th thoracic spine; L4, the 4th lumbar spinal cords.

Another interesting finding in our study is that both EA and PGB were able to relieve painful hypersensitivity in SNI rats. However, EA interventions could also restore the normal structures, while PGB treatment did not show any improvement. This was also consistent with our previous studies. These results imply that neuromodulation techniques have additional advantages when compared to a pharmacologic approach in the treatment of chronic pain. EA, a therapeutic means based on acupuncture combined with electrical stimulation,[39] has proven effective in pain relief[40] and multiple organ protection.[41] Parmen et al[42] showed that EA can facilitate an improvement in tissue mechanical stress and enhance the wound healing process without detrimental side effects. In addition, EA can also promote tissue repair, ultrastructural reconstruction and pain relief by reducing neuronal apoptosis,[43] inhibiting the spinal glial cell activation[40] and neuroinflammatory response,[44] decreasing cytokines and mediating the release of mesenchymal stem cells.[45] Conversely, PGB administration did not affect the ultrastructural changes, although it did show a beneficial effect on pain relief in the SNI rat model. Unfortunately, it is unclear what the possible mechanism is for this interesting phenomenon even though we carefully consulted the literature.

This study has several flaws and limitations. Firstly, the systemic ultrastructural alterations were observed at different levels of the nervous system in SNI rat. However, we are not explicitly aware of the detailed timeline of the damage process. For example, we cannot establish with certainty if the spinal cord damage preceded or followed the onset of the brain changes. Secondly, the morphological study was a non-quantitative and observational study. A quantitative study is the direction for our future work. Thirdly, there were inadequate numbers of dorsal horn neuron images suitable for direct comparison. Fourthly, we do not know the precise molecular and biological mechanism of the micro-structural changes induced by our chronic pain model. Fifthly, although we found several meaningful outcome changes, the significance behind these phenomena is unknown. We can only surmise that

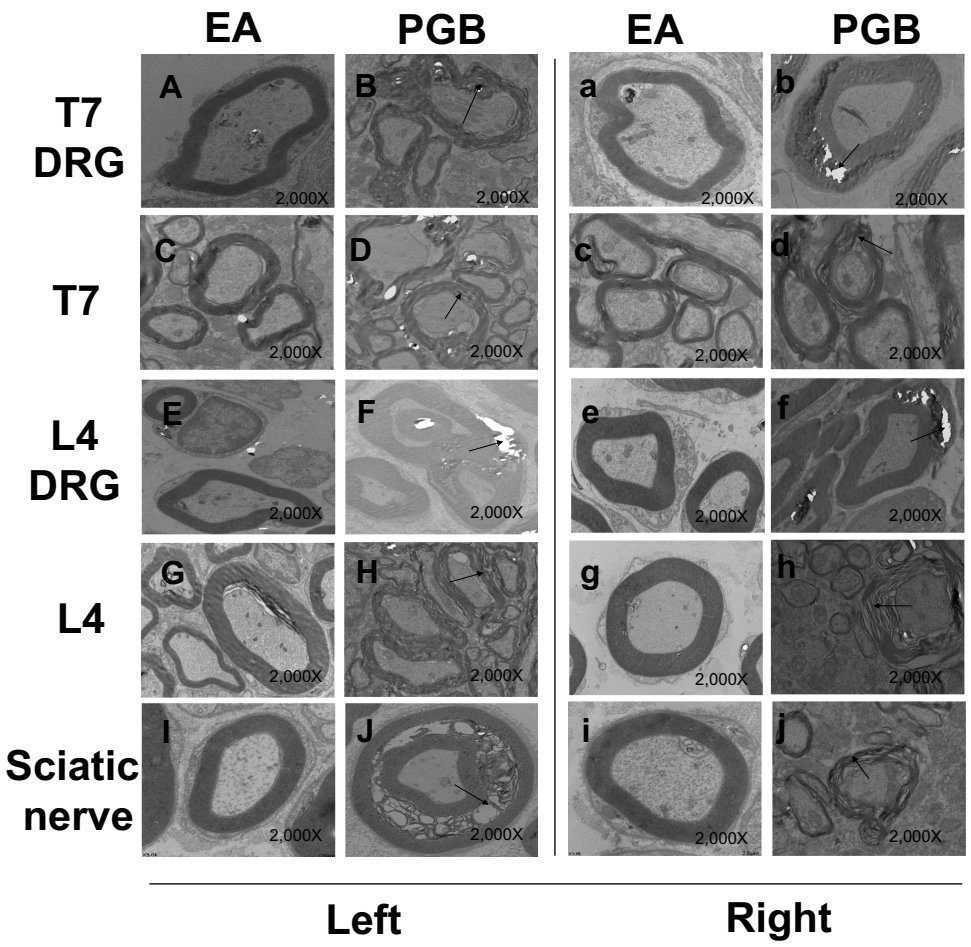

Figure 9 Ultrastructural changes of thoracic and lumbar spine, DRGs and sciatic nerves in EA and PGB group.
Notes: TEM observations show that myelin sheaths on the operative and non-operative thoracic, lumbar spinal cords levels, DRGs and sciatic nerves are intact and normal in EA group (**A, a, C, c, E, e, G, g, I, i**). However, partial myeloid dissolution and onion-like demyelinating changes are still observed in PGN group (**B, b, D, d, F, f, H, h, J, j**). (**A, a, C, c, E, e, G, g, I**, (i) show the ultrastructural changes of thoracic and lumbar spine, DRGs and sciatic nerves in EA group. (**A, C, E, G, I**) represent the left side (operative side). While **a, c, e, g, I** represent the right side (non-operative side). (**B, b, D, d, F, f, H, h, J, j**) represent the ultrastructural changes of thoracic and lumbar spine, DRGs and sciatic nerves in SNI group. (**B, D, F, H, J**) represent the left side (operative side). While (**b, d, f, h, j**) represent the right side (non-operative side).
Abbreviations: SNI, spared nerve injury; EA, electroacupuncture; PGB, pregabalin; T7, the 7th thoracic spine; L4, the 4th lumbar spinal cords; DRG, dorsal root ganglion.

many of the mental health disorders induced by chronic pain are partially explained by the systemic ultrastructural alterations of the nervous systems. Future research should also aim to specifically address these questions. Sixthly, we have no information as to whether the pathological changes we observed in the present study were due to tearing of the tissue or vacuolization during preparation of the tissues. Finally, only the mechanical withdrawal thresholds (MWTs) were assessed in this study. Thermal and cold hyperalgesia were not assessed among groups.

Conclusion

Chronic pain can induce extensive damage to the central and peripheral nervous systems. Meanwhile, both EA and PGB can alleviate chronic pain syndrome, but EA also restores the normal structures, while PGB is associated with no improvement.

Abbreviations

SNI, nerve injury group; EA, electroacupuncture; PGB, pregabalin; NP, neuropathic pain; CNS, central nervous system; MCC, mid-cingulate cortex; TN, trigeminal neuralgia; PFC, prefrontal cortex; CCI, chronic contractile injury; DRGs, dorsal root ganglions; SD, standard deviation; ANOVA, one-way analysis of variance; SNL, spinal nerve ligation model; IL-10, interleukin-10; MCP-1, monocyte chemoattractant protein-1.

Funding

This study was supported by National Natural Science Foundation of China, Beijing, China. (81671076).

Disclosure

Lei Gao & Jian-Feng Zhang are co-first authors for this study. The authors report no conflicts of interest in this work.

References

1. Smith BH, Hébert HL, Veluchamy A. Neuropathic pain in the community: prevalence, impact, and risk factors. *Pain*. 2020;161(Suppl Supplement 1):S127–S137. doi:10.1097/j.pain.0000000000001824
2. Ma X, Du W, Wang W, et al. Persistent Rheb-induced mTORC1 activation in spinal cord neurons induces hypersensitivity in neuropathic pain. *Cell Death Dis*. 2020;11(9):747. doi:10.1038/s41419-020-02966-0
3. Tigerholm J, Poulsen AH, Andersen OK, Mørch CD. From perception threshold to ion channels-A computational study. *Biophys J*. 2019;117(2):281–295. doi:10.1016/j.bpj.2019.04.041
4. Castellanos JP, Woolley C, Bruno KA, Zeidan F, Halberstadt A, Furnish T. Chronic pain and psychedelics: a review and proposed mechanism of action. *Reg Anesth Pain Med*. 2020;45(7):486–494. doi:10.1136/rapm-2020-101273
5. Bannister K, Sachau J, Baron R, Dickenson AH. Neuropathic pain: mechanism-based therapeutics. *Annu Rev Pharmacol Toxicol*. 2020;60(1):257–274. doi:10.1146/annurev-pharmtox-010818-021524
6. Sobeh M, Mahmoud MF, Rezq S, et al. Salix tetrasperma Roxb. extract alleviates neuropathic pain in rats via modulation of the NF-κB/TNF-α/NOX/iNOS pathway. *Antioxidants*. 2019;8:10.
7. Seminowicz DA, Moayedi M. The dorsolateral prefrontal cortex in acute and chronic pain. *J Pain*. 2017;18(9):1027–1035. doi:10.1016/j.jpain.2017.03.008
8. Duerden EG, Albanese MC. Localization of pain-related brain activation: a meta-analysis of neuroimaging data. *Hum Brain Mapp*. 2013;34(1):109–149. doi:10.1002/hbm.21416
9. Etkin A, Büchel C, Gross JJ. The neural bases of emotion regulation. *Nat Rev Neurosci*. 2015;16(11):693–700. doi:10.1038/nrn4044
10. Wang Y, Cao DY, Remeniuk B, Krimmel S, Seminowicz DA, Zhang M. Altered brain structure and function associated with sensory and affective components of classic trigeminal neuralgia. *Pain*. 2017;158(8):1561–1570. doi:10.1097/j.pain.0000000000000951
11. Chen RW, Liu H, An JX, et al. Cognitive effects of electro-acupuncture and pregabalin in a trigeminal neuralgia rat model induced by cobra venom. *J Pain Res*. 2017;10:1887–1897. doi:10.2147/JPR.S140840
12. Wu Z, Qian XY, An JX, et al. Trigeminal neuralgia induced by cobra venom in the rat leads to deficits in abilities of spatial learning and memory. *Pain Physician*. 2015;18(2):E207–E216.
13. Zhao QQ, Qian XY, An JX, et al. Rat model of trigeminal neuralgia using cobra venom mimics the electron microscopy, behavioral, and anticonvulsant drug responses seen in patients. *Pain Physician*. 2015;18(6):E1083–E1090.
14. Zimmermann M. Ethical guidelines for investigations of experimental pain in conscious animals. *Pain*. 1983;16(2):109–110. doi:10.1016/0304-3959(83)90201-4
15. Decosterd I, Woolf CJ. Spared nerve injury: an animal model of persistent peripheral neuropathic pain. *Pain*. 2000;87(2):149–158. doi:10.1016/S0304-3959(00)00276-1
16. Chaplan SR, Bach FW, Pogrel JW, Chung JM, Yaksh TL. Quantitative assessment of tactile allodynia in the rat paw. *J Neurosci Methods*. 1994;53(1):55–63. doi:10.1016/0165-0270(94)90144-9
17. Lu GF, Zhang JM, An JX, et al. Enhanced pain sensitivity with systemic ultrastructural changes of the nervous systems after cobra venom injection is reversed by electroacupuncture treatment. *Pain Physician*. 2018;21(5):E509–E521.
18. Lao L, Zhang RX, Zhang G, Wang X, Berman BM, Ren K. A parametric study of electroacupuncture on persistent hyperalgesia and Fos protein expression in rats. *Brain Res*. 2004;1020(1–2):18–29. doi:10.1016/j.brainres.2004.01.092
19. Gao YH, Chen SP, Wang JY, et al. Differential proteomics analysis of the analgesic effect of electroacupuncture intervention in the hippocampus following neuropathic pain in rats. *BMC Complement Altern Med*. 2012;12(1):241. doi:10.1186/1472-6882-12-241
20. Zhang N, Li JL, Yan CQ, et al. The cerebral mechanism of the specific and nonspecific effects of acupuncture based on knee osteoarthritis: study protocol for a randomized controlled trial. *Trials*. 2020;21(1):566. doi:10.1186/s13063-020-04518-5
21. Zhang YT, Jin H, Wang JH, et al. Tail nerve electrical stimulation and electro-acupuncture can protect spinal motor neurons and alleviate muscle atrophy after spinal cord transection in rats. *Neural Plast*. 2017;2017:7351238. doi:10.1155/2017/7351238
22. Apkarian AV, Bushnell MC, Treede RD, Zubieta JK. Human brain mechanisms of pain perception and regulation in health and disease. *Eur J Pain*. 2005;9(4):463–484.
23. Bennett GJ, Xie YK. A peripheral mononeuropathy in rat that produces disorders of pain sensation like those seen in man. *Pain*. 1988;33(1):87–107. doi:10.1016/0304-3959(88)90209-6
24. Chung JM, Kim HK, Chung K. Segmental spinal nerve ligation model of neuropathic pain. *Methods Mol Med*. 2004;99:35–45.
25. Shiers S, Mwirigi J, Pradhan G, et al. Reversal of peripheral nerve injury-induced neuropathic pain and cognitive dysfunction via genetic and tomivosertib targeting of MNK. *Neuropsychopharmacology*. 2020;45(3):524–533. doi:10.1038/s41386-019-0537-y
26. Guan Z, Kuhn JA, Wang X, et al. Injured sensory neuron-derived CSF1 induces microglial proliferation and DAP12-dependent pain. *Nat Neurosci*. 2016;19(1):94–101. doi:10.1038/nn.4189
27. Wlaschin JJ, Gluski JM, Nguyen E, et al. Dual leucine zipper kinase is required for mechanical allodynia and microgliosis after nerve injury. *Elife*. 2018;7:e33910.
28. Chang MC, Park D. Effectiveness of intravenous immunoglobulin for management of neuropathic pain: a narrative review. *J Pain Res*. 2020;13:2879–2884. doi:10.2147/JPR.S273475
29. Ji RR, Berta T, Nedergaard M. Glia and pain: is chronic pain a gliopathy? *Pain*. 2013;154(Suppl 1):S10–S28.
30. Basbaum AI, Bautista DM, Scherrer G, Julius D. Cellular and molecular mechanisms of pain. *Cell*. 2009;139(2):267–284. doi:10.1016/j.cell.2009.09.028
31. Bäckryd E, Lind AL, Thulin M, Larsson A, Gerdle B, Gordh T. High levels of cerebrospinal fluid chemokines point to the presence of neuroinflammation in peripheral neuropathic pain: a cross-sectional study of 2 cohorts of patients compared with healthy controls. *Pain*. 2017;158(12):2487–2495. doi:10.1097/j.pain.0000000000001061
32. Ji RR, Nackley A, Huh Y, Terrando N, Maixner W. Neuroinflammation and central sensitization in chronic and widespread pain. *Anesthesiology*. 2018;129(2):343–366.
33. Woolf CJ, Salter MW. Neuronal plasticity: increasing the gain in pain. *Science*. 2000;288(5472):1765–1769. doi:10.1126/science.288.5472.1765
34. Ueda H. Peripheral mechanisms of neuropathic pain - involvement of lysophosphatidic acid receptor-mediated demyelination. *Mol Pain*. 2008;4:11. doi:10.1186/1744-8069-4-11
35. Kleinschnitz C, Brinkhoff J, Sommer C, Stoll G. Contralateral cytokine gene induction after peripheral nerve lesions: dependence on the mode of injury and NMDA receptor signaling. *Brain Res Mol Brain Res*. 2005;136(1–2):23–28. doi:10.1016/j.molbrainres.2004.12.015
36. Koltzenburg M, Wall PD, McMahon SB. Does the right side know what the left is doing? *Trends Neurosci*. 1999;22(3):122–127. doi:10.1016/S0166-2236(98)01302-2
37. Jancálek R, Dubový P, Svízenská I, Klusáková I. Bilateral changes of TNF-alpha and IL-10 protein in the lumbar and cervical dorsal root ganglia following a unilateral chronic constriction injury of the sciatic nerve. *J Neuroinflammation*. 2010;7(1):11. doi:10.1186/1742-2094-7-11

38. Kleinschnitz C, Brinkhoff J, Zelenka M, Sommer C, Stoll G. The extent of cytokine induction in peripheral nerve lesions depends on the mode of injury and NMDA receptor signaling. *J Neuroimmunol*. 2004;149(1–2):77–83. doi:10.1016/j.jneuroim.2003.12.013
39. Yeh BY, Liu GH, Lee TY, Wong AM, Chang HH, Chen YS. Efficacy of electronic acupuncture shoes for chronic low back pain: double-blinded randomized controlled trial. *J Med Internet Res*. 2020;22(10):e22324. doi:10.2196/22324
40. Zhang R, Lao L, Ren K, Berman BM. Mechanisms of acupuncture-electroacupuncture on persistent pain. *Anesthesiology*. 2014;120(2):482–503. doi:10.1097/ALN.0000000000000101
41. Jia L, Yu W, Yu H, Weng Y. Electroacupuncture pretreatment attenuates intestinal injury after autogenous orthotopic liver transplantation in rats via the JAK/STAT pathway. *Oxid Med Cell Longev*. 2020;2020:9187406. doi:10.1155/2020/9187406
42. Parmen V, Taulescu M, Ober C, Pestean C, Oana L. Influence of electroacupuncture on the soft tissue healing process. *J Acupunct Meridian Stud*. 2014;7(5):243–249. doi:10.1016/j.jams.2014.03.003
43. Wu MF, Zhang SQ, Liu JB, Li Y, Zhu QS, Gu R. Neuroprotective effects of electroacupuncture on early- and late-stage spinal cord injury. *Neural Regen Res*. 2015;10(10):1628–1634. doi:10.4103/1673-5374.167762
44. Hong ES, Yao HH, Min YJ, et al. The mechanism of electroacupuncture for treating spinal cord injury rats by mediating Rho/Rho-associated kinase signaling pathway. *J Spinal Cord Med*. 2019;44:1–11.
45. Salazar TE, Richardson MR, Beli E, et al. Electroacupuncture promotes central nervous system-dependent release of mesenchymal stem cells. *Stem Cells*. 2017;35(5):1303–1315. doi:10.1002/stem.2613